

High Resolution K Capture X-ray Fluorescence Spectroscopy: A New Tool for Chemical Characterization

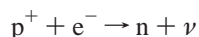
U. Bergmann,[†] P. Glatzel,[‡] F. deGroot,[§] and S. P. Cramer^{*,†,‡}

Physical Biosciences Division
Lawrence Berkeley National Laboratory
Berkeley, California 94720
Department of Applied Science
University of California
Davis, California 95616
Department of Chemistry
Universiteit Utrecht
3584 CA Utrecht, The Netherlands

Received December 29, 1998

The ability to probe specific chemical sites in complex systems would make X-ray spectroscopy a far more versatile spectroscopic tool. In vibrational and magnetic resonance spectroscopies, isotopic substitution is commonly employed to allow characterization of particular species. Except in a few special cases, such as gas-phase spectra of light elements, isotope effects are too small to be observed in X-ray absorption spectra. An alternative approach is to examine the X-ray emission that results after electron capture by a radioactive isotope.^{1,2} Controlled introduction of electron-capture isotopes could result in specific labeling of chemically distinct sites. In this paper, we show that high-resolution electron capture fluorescence spectra can be obtained on a reasonable time scale. Chemical shifts in these spectra can be used to identify elemental spin states, oxidation states, and even the types of neighboring atoms.

In the electron-capture process an inner shell electron reacts with a nuclear proton to yield a neutron and a neutrino¹



For an element with atomic number Z , the 1s vacancy that is produced by K-capture is similar to that created in K-edge X-ray absorption, except that the nucleus now has charge $Z - 1$. Just as with X-ray excited emission, the core hole is subsequently filled by a higher level electron, and the extra energy is released by emission of an Auger electron or X-ray fluorescence. $K\alpha$ X-ray fluorescence results from $2p \rightarrow 1s$ transitions, while $K\beta$ X-ray fluorescence results when the 1s core hole is filled from orbitals with 3p or 4p character.

$K\beta$ X-ray fluorescence is often split by a 3p–3d exchange interaction into a strong $K\beta_{1,3}$ region and a weaker $K\beta'$ satellite.³ Chemical shifts in Mn $K\beta_{1,3}$ lines⁴ have been used to record site-selective EXAFS of different Mn oxidation states in mixed valence complexes⁵ and to identify the mixtures of Mn oxidation states in photosystem II.⁶ The $K\beta_{2,5}$ region has also been shown to shift with oxidation state.⁷

K-capture spectra for ⁵⁵Fe metal and ⁵⁵Fe₂O₃ are compared with X-ray excited $K\beta$ emission spectra for Mn metal and MnO in

Figure 1.⁸ The measurements⁹ were done at NSLS beamline X-25¹⁰ and SSRL beamline 10-2¹¹ using a crystal array spectrometer.^{12,13} The Mn metal spectrum exhibits a $K\beta_{1,3}$ peak at 6490.6 eV, and it has a broad, structureless tail extending ~20 eV to lower energy. The MnO spectrum has a $K\beta_{1,3}$ peak shifted 1.4 eV to higher energy, and a $K\beta'$ maximum at 6477 eV. Similar spectra have been reported for other Mn(II) complexes.⁴ The large $K\beta_{1,3}$ – $K\beta'$ splitting for Mn(II) is attributed to a strong 3p–3d exchange interaction for high-spin 3d⁵ materials.³

The ⁵⁵Fe metal K capture spectrum resembles that of the X-ray excited Mn foil, and we find that the $K\beta_{1,3}$ peaks are located at the same energy, in contrast to a previous report that found a 0.6 eV shift.¹⁴ The capture spectrum $K\beta_{1,3}$ peak is measurably sharper (fwhm ≈ 3.0 vs 3.6 eV). One essential difference between the two modes of excitation involves the effect of the core hole on the valence electron distribution. Upon X-ray excitation of a 3d^N metal complex, the presence of a core hole lowers the energy of the metal valence orbitals. The intermediate state can be expressed as $1s^1 3d^N$ and an appreciable fraction of $1s^1 3d^{N+1} \underline{L}$, where \underline{L} represents a ligand hole. The $1s^1 3d^{N+1} \underline{L}$ component gives rise to additional fluorescence transitions which broaden the X-ray spectrum. In contrast, after K-capture the 1s vacancy and the lower nuclear charge approximately cancel, the intermediate electronic configuration remains primarily $1s^1 3d^N$, and the result is a sharper spectrum.

It has been suggested that fewer multielectron excitations occur during K-capture as opposed to X-ray excitation.¹⁵ Bianconi and co-workers have documented 2-electron excitations in Mn complexes,¹⁶ and fluorescence from these channels would be expected at different energies from the normal $K\beta$ features.

(6) Bergmann, U.; Grush, M. M.; Horne, C. R.; DeMarois, P.; Penner-Hahn, J. E.; Yocum, C. F.; Wright, D. W.; Dube, C. E.; Armstrong, W. H.; Christou, G.; Eppley, H. J.; Cramer, S. P. *J. Phys. Chem. B* **1998**, *102*, 8350–8352.

(7) Bergmann, U.; Horne, C. R.; Collins, T. J.; Cramer, S. P. *Chem. Phys. Lett.* **1999**, *302*, 119–124.

(8) MnO (99.5%) was obtained from Alfa/AESAR, and Mn metal powder (>99%, –325 mesh) was from Aldrich. The ⁵⁵Fe metal samples were standard sources supplied by New England Nuclear. ⁵⁵Fe₂O₃ was prepared by spiking 0.05 mL of ⁵⁵Fe ferric nitrate solution (45.3 mCi/mL) (NEN Life Science Products) into 13.6 mg of stable reagent grade Fe(NO₃)₃·9H₂O dissolved in 1 mL of H₂O. NH₄OH (2 M) was added dropwise to complete the Fe(OH)₃ precipitation. The Fe(OH)₃ precipitate was centrifuged, washed twice with 2 mL of H₂O, dried under a heat lamp, and heated further to cause transformation to Fe₂O₃. The sample activities used for spectroscopy were 5 mCi for the ⁵⁵Fe metal and 0.5 mCi for ⁵⁵Fe₂O₃.

(9) The X-ray excited spectra were recorded at the NSLS, with a 6700 eV incident beam energy. The incident flux (I_0) was recorded with an air-filled ion chamber, and the spectra were corrected for changes in I_0 . The incident beam flux was on the order of order 10¹² photons/s. The samples were at room temperature during data collection. ⁵⁵Fe metal K-capture fluorescence spectra were recorded at both X-25 and 10-2, while the ⁵⁵Fe₂O₃ spectrum was recorded both at SSRL and at UC Davis. Near the $K\beta$ maximum, the count rates were ~60 cts/s for the ⁵⁵Fe and ~10 cts/s for the ⁵⁵Fe₂O₃ spectra.

(10) Berman, L. E.; Hastings, J. B.; Oversluisen, T.; Woodle, M. *Rev. Sci. Instrum.* **1992**, *63*, 428–432.

(11) Karpenko, V.; Kinney, J. H.; Kulkarni, S.; Neufeld, K.; Poppe, C.; Tirsell, K. G.; Wong, J.; Cerino, J.; Troxel, T. J. *Y. Rev. Sci. Instrum.* **1989**, *60*, 1451–1456.

(12) The fluorescence spectrometer for the current experiments used eight 8.9-cm diameter Si(440) analyzer crystals aligned on Rowland circles with respect to sample and detector, and they captured a total solid angle of 0.07 sr. A He-filled bag enclosed the entire emitted beam path. The energy resolution was approximately 0.7 eV (at 6470 eV) and 1.5 eV (at 6560 eV). The instrument was calibrated by measuring the absolute angle of the Bragg reflection. In a previous study of ⁵⁵Fe spectra, the count rate was 100-fold lower with a source that was 200-fold stronger.¹⁵

(13) Bergmann, U.; Cramer, S. P. *SPIE Proc.* **1998**, *3448*, 198–209.

(14) Dem'yanchuk, A. V.; Zhmudskiy, A. Z.; Surzhko, V. F.; Shiyanyovskiy, V. I. *Fiz. Met. Metalloved.* **1977**, *43*, 1307–1308.

(15) Schnopper, H. W.; Parratt, L. G. In *Röntgenspektren und Chemische Bindung*; Meisel, A., Ed.; Leipzig University Press: Leipzig, 1966; pp 314–324.

(16) Bianconi, A.; Garcia, J. M. B.; Marcelli, A.; Natoli, C. R.; Ruiz Lopez, M. F. *Phys. Rev. B* **1991**, *43*, 6885–6892.

* To whom the correspondence should be addressed.

[†] Lawrence Berkeley National Laboratory.

[‡] University of California at Davis.

[§] Universiteit Utrecht.

(1) Marmier, P.; Sheldon, E. *Physics of Nuclei and Particles*; Academic Press: New York, 1969; Vol. I.

(2) Konopinski, E. J. *The Theory of Beta Radioactivity*; Oxford University Press: London, 1966

(3) Ekstig, B.; Kallne, E.; Noreland, E.; Manne, R. *Phys. Scr.* **1970**, *2*, 38–44.

(4) Peng, G.; Degroot, F. M. F.; Hämmäläinen, K.; Moore, J. A.; Wang, X.; Grush, M. M.; Hastings, J. B.; Siddons, D. P.; Armstrong, W. H.; Mullins, O. C.; Cramer, S. P. *J. Am. Chem. Soc.* **1994**, *116*, 2914–2920.

(5) Grush, M. M.; Christou, G.; Hämmäläinen, K.; Cramer, S. P. *J. Am. Chem. Soc.* **1995**, *117*, 5895–5896.

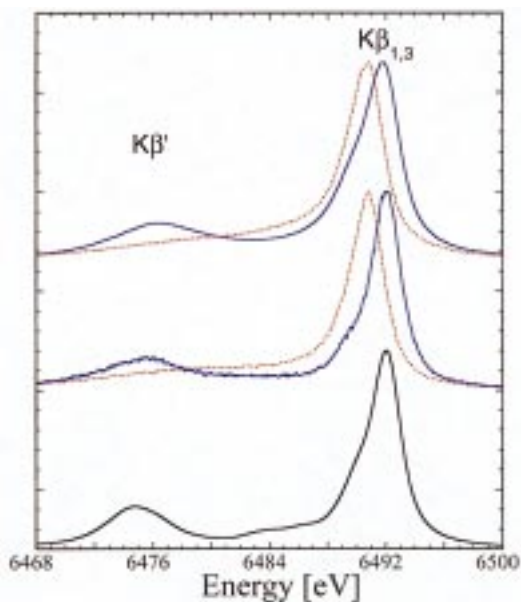


Figure 1. Comparison of X-ray excited and K-capture $K\beta$ emission spectra. Top to bottom: (a) X-ray excited $K\beta_{1,3}$ spectra for MnO (blue line) vs Mn metal (red dashes); (b) K-capture $K\beta$ spectra for $^{55}\text{Fe}_2\text{O}_3$ (blue line) and Fe metal (red dashes); (c) a ligand field multiplet simulation with $10Dq = 2.4$ eV.⁴

Reduction or elimination of multielectron excitations may also be a factor in the narrower line widths.

The K-capture $K\beta$ spectrum for $^{55}\text{Fe}_2\text{O}_3$ is also sharper than that of the X-ray excited analogue, and the $K\beta_{1,3}$ peak shows a 1.5 eV shift to higher energy from ^{55}Fe metal. The $K\beta_{1,3}$ peak has a weak shoulder on the low-energy side, and there is a clear $K\beta'$ feature at about 17 eV lower energy. These features are qualitatively reproduced by a ligand field multiplet simulation for a d^5 configuration with $10Dq = 2.4$ eV.⁴ To our knowledge, this is the first observation of significant chemical shifts and spectral intensity changes in K capture spectra. The strength and energy of the $K\beta'$ feature suggests that on the femtosecond time scale of this experiment, the new ($1s^1$) ^{55}Mn ion maintains a high-spin d^5 valence configuration after K-capture.

Figure 2 compares the higher energy range containing the $K\beta''$ and $K\beta_{2,5}$ features. The latter region has been assigned to dipole transitions from molecular orbitals with some Mn 4p character and to $3d \rightarrow 1s$ quadrupole transitions.^{17–20} Both oxide spectra show structure in the $K\beta_{2,5}$ region, and the major features can be fit with 2 Gaussians separated by ~ 3 eV (Figure 2). In a molecular orbital scheme for octahedral complexes, the ligand p orbitals transform with t_{1g} , t_{2g} , t_{1u} , and t_{2u} character.²¹ The dipole operator transforms as t_{1u} ,²² and there are two t_{1u} symmetry ligand orbitals, formed from oxygen $p(\pi)$ and $p(\sigma)$ orbitals, that can mix with the t_{1u} metal 4p orbitals.²³ We assign the main peak and lower energy shoulder in the $K\beta_{2,5}$ spectrum to transitions from these orbitals. There is additional structure on the high-energy side of

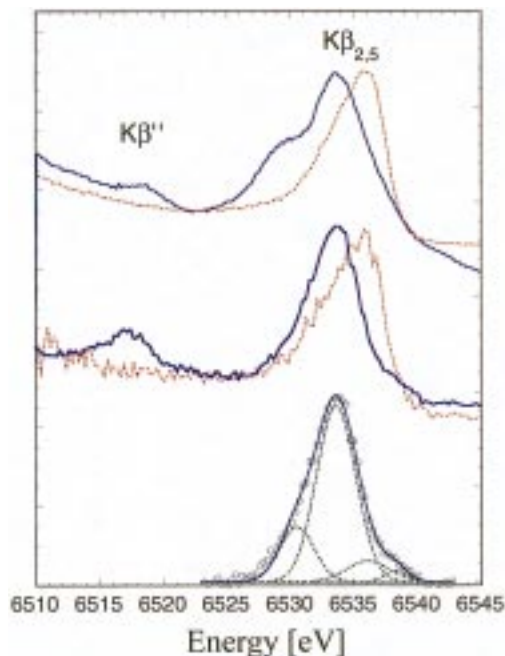


Figure 2. Valence band $K\beta$ emission spectra. Top to bottom: (a) X-ray excited $K\beta_{2,5}$ and $K\beta''$ spectra for MnO (blue line) vs Mn metal (red dashes); (b) K-capture $K\beta_{2,5}$ and $K\beta''$ spectra for $^{55}\text{Fe}_2\text{O}_3$ (blue line) and Fe metal (red dashes); (c) a fit of the background-subtracted $K\beta_{2,5}$ region with 4 Gaussians.

the $K\beta_{2,5}$ feature which can be fit with 2 Gaussians separated by ~ 2.2 eV. We assign this structure to $3d \rightarrow 1s$ quadrupole transitions. The 2.2 eV splitting is consistent with the $10Dq$ value used in the simulation and with $d-d$ splittings observed in Fe_2O_3 photoelectron spectra.²⁴ Finally, at ~ 22 eV below the emission threshold, the oxide spectra exhibit $K\beta''$ features that correspond to oxygen $2s [t_{1u}(\sigma)] \rightarrow \text{Mn } 1s$ “crossover” transitions.⁷ It is clear that the K-capture spectrum reveals a wealth of information about the valence energy levels in an inorganic complex.

In conclusion, we have demonstrated for the first time the significant chemical sensitivity of K-capture $K\beta$ spectra. On the basis of known fluorescence chemical shifts, this technique shows potential for characterization of oxidation states,⁴ spin states,^{4,25} and even ligand type⁷ for specific sites in heterogeneous samples. Because hard X-rays are used, K-capture methods could be especially valuable for chemical characterization of surfaces under catalytically relevant conditions. When the biochemistry permits, labeling of individual metal sites in multinuclear enzymes might also prove useful. Finally, K-capture spectroscopy should be a useful probe of valence electronic structure, with less core hole influence than conventional X-ray emission.

Acknowledgment. We especially thank Dr. Sandra Fadeff at Pacific Northwest National Labs for preparing the $^{55}\text{Fe}_2\text{O}_3$ sample. This research was supported by the National Institutes of Health, Grants 44891-5 and GM-48145 (to S.P.C.) and by the Department of Energy, Office of Biological and Environmental Research. The National Synchrotron Light Source and the Stanford Synchrotron Radiation Laboratory are supported by the Department of Energy, Office of Basic Energy Sciences.

JA984454W

(17) Best, P. E. *Chem. Phys.* **1966**, *44*, 3248–3253.

(18) Urch, D. S. In *Electron Spectroscopy: Theory, Techniques, and Application*; Brundle, C. R., Baker, A. D., Eds.; Academic Press: New York, 1979; Vol. 3, pp 1–39.

(19) Koster, A. S.; Mendel, H. *Phys. Chem. Solids* **1970**, *31*, 2511–2522.

(20) Tsutsumi, K.; Nakamori, H.; Ichikawa, K. *Phys. Rev. B* **1976**, *13*, 929–933.

(21) Ballhausen, C. J.; Gray, H. B. *Molecular Orbital Theory*; Benjamin: New York, 1964.

(22) Cotton, F. A. *Chemical Applications of Group Theory*; Wiley: New York, 1990.

(23) Lever, A. B. P. *Inorganic Electronic Spectroscopy*; Elsevier: Amsterdam, 1984.

(24) Fujimori, A.; Saeki, M.; Kimizuka, N. *Phys. Rev. B* **1986**, *34*, 7318–7328.

(25) Wang, X.; Randall, C. R.; Peng, G.; Cramer, S. P. *Chem. Phys. Lett.* **1995**, *243*, 469–473.